

# Layering instability in a confined suspension flow

M. Zurita-Gotor,<sup>1</sup> J. Bławdziewicz,<sup>2</sup> and E. Wajnryb<sup>3</sup>

<sup>1</sup>*Departamento de Ingeniería Aeroespacial y Mecánica de Fluidos, Universidad de Sevilla, Sevilla 41092, Spain*

<sup>2</sup>*Department of Mechanical Engineering, Texas Tech University, Lubbock, Texas 79409, USA*

<sup>3</sup>*Institute of Fundamental Technological Research, Warsaw, Polish Academy of Sciences*

(Dated: November 6, 2018)

We have shown [J. Fluid Mech. **592**, 447 (2007)] that swapping (reversing) trajectories in confined suspension flows prevent collisions between particles approaching each other in adjacent streamlines. Here we demonstrate that by inducing layering this hydrodynamic mechanism changes the microstructure of suspensions in a confined Couette flow. Layers occur either in the near-wall regions or span the whole channel width, depending on the strength of the swapping-trajectory effect. While our theory focuses on dilute suspensions, we postulate that this new hydrodynamic mechanism controls formation of a layered microstructure in such flows in a wide range of densities.

PACS numbers: xxxx

Confined particulate flows are important due to their applications in microfabrication, microfluidics and biotechnology. Recent studies have shown complex non-linear microstructural evolution [1–7], strikingly different than the behavior with no confining walls.

Confinement affects the system behavior both by imposing geometrical constraints on particle motion and by giving rise to purely hydrodynamic mechanisms. While geometry-driven phenomena have been extensively studied (e.g., ordered structures in dense suspensions and emulsions tightly confined by bounding walls [1]), hydrodynamic mechanisms that are wall-induced have only recently been at the center of attention.

So far the most thoroughly investigated hydrodynamic confinement phenomenon is the fluid backflow produced by particle motion. It has been studied in linear conduits [8, 9], and in parallel-wall channels [3, 10]. The backflow gives rise to the anomalous sign of the mutual diffusion coefficient for Brownian spheres [3, 10], wave propagation in flow-driven drop or particle trains [4, 5, 7], and unusual stability of a square particle lattice [5, 7].

Here we demonstrate that the evolution of suspension microstructure also depends on the swapping (reversing) trajectory effect [11, 12]. Because this proposed confinement-induced hydrodynamic mechanism prevents collisions of particles in adjacent streamlines in a confined Couette flow, a uniform suspension microstructure is destabilized, leading to the formation of particle layers parallel to the walls (cf., Figs. 1 and 2).

Layered suspension microstructure that spontaneously arises in confined flows, even at moderate particle concentrations, has recently been observed experimentally [13] and in computer simulations [2] (also in movies A1–A4 in [14]). A key hydrodynamic mechanism responsible for this behavior is revealed by our present work.

We consider a suspension of non-Brownian spherical particles in planar Couette flow of shear rate  $\dot{\gamma}$  [cf., Fig. 1(a)], under creeping-flow conditions. The particles have finite roughness, which is modeled by a very steep, short-

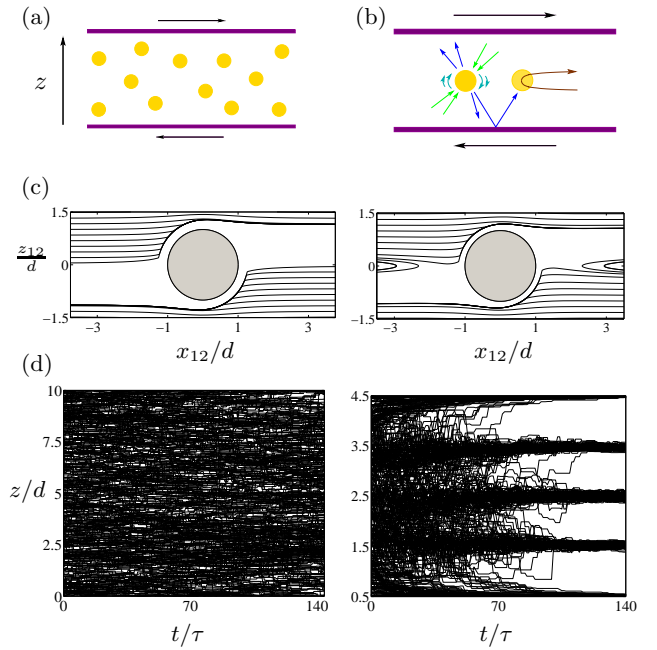


FIG. 1. Wall-induced layering. (a) Suspension geometry. (b) Swapping-trajectory (ST) effect: the flow scattered from the walls produces lift causing the reversal of particle motion. (c) Relative particle trajectories in two systems: unconfined (left) and confined with an ST region (right). (d) Time evolution of the transverse position  $z$  in suspension: unconfined (left) and confined (right). Time is normalized by the characteristic time between collisions  $\tau = 1/(n_0 \dot{\gamma} d^3)$ .

range repulsive potential of the range  $d_r = d + \epsilon$  (where  $d$  is the hydrodynamic diameter) to mimic contacts between roughness asperities. These direct particle contacts remove the Stokes-flow symmetry of binary collisions, producing finite transverse particle displacements [15], as illustrated in Fig. 1(c).

Our analysis is focused on the dilute-suspension limit. The simulations in Figs. 1 and 2 are performed using the Boltzmann–Monte Carlo (BMC) method, in which the

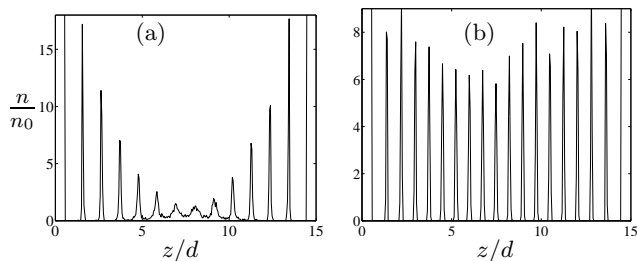


FIG. 2. Suspension microstructure for particles of different roughness in a channel of width  $H/d = 15$  at time  $t/\tau = 2400$ . Density profiles  $n/n_0$  are shown vs transverse position  $z/d$ . Roughness range (a)  $\epsilon/d = 0.25$ ; (b)  $\epsilon/d = 0.064$ .

system dynamics is modeled as a sequence of uncorrelated binary collisions [11]. Since particle correlations are important only at higher concentrations, this approach is appropriate in the low-concentration regime. We analyze suspensions at low concentrations  $n_0$  to emphasize physical mechanisms involved in the formation of the layered microstructure. However, our direct numerical simulations (cf., movies B1-B4 in [14]) demonstrate that these mechanisms are present also at higher concentrations.

In the BMC method, the particle distribution is evolved by performing a sequence of uncorrelated collisional steps. In each step, we choose a random pair of particles, simulate their binary collision, and update the cross-streamline particle positions according to the post-collisional displacements [14]. When binary trajectories are accurately evaluated taking into account the hydrodynamic interactions (HI) in the wall presence [10, 14], we refer to this description as BMC-HI. To highlight the role of topological features of pair trajectories without incurring large numerical cost of evaluation of HI, we use two simplified collision models M2 and M3 (described below). Figures 1 and 2 were obtained using BMC-HI, and Figs. 3–6 correspond to models M2 and M3.

Figure 1(d) demonstrates that a suspension confined between two parallel walls develops a well-defined layered structure (after about 20 collisions per particle), while the unconfined system remains uniform. Fig. 2 illustrates a strong dependence of the layered structure on the range  $\epsilon$  of non-hydrodynamic interparticle interactions.

We argue that the observed layering behavior stems from the swapping-trajectory (ST) effect that causes approaching particles to reverse their motion, and avoid collision. Such trajectories, which occur in the wall presence [cf., Fig. 1(c)], prevent large collisional displacements for particles with a sufficiently small transverse offset, leading, therefore, to stabilization of particle layers.

The ST domain results from wall-mediated HI between the approaching particles [11]. The wall reflection of the perturbation flow produced by one of the particles [cf., Fig. 1(b)] pushes the other particle across streamlines of the applied flow toward the fluid moving in the oppo-

site direction, causing the reversal of the relative particle motion. Through this purely hydrodynamic mechanism confining walls influence the suspension microstructure.

*Population-balance equation* – To elucidate the effect of swapping trajectories on the suspension dynamics we use the population-balance method, where the particle density  $n(z)$  (uniform in the flow and vorticity directions  $x$  and  $y$ ) is described by a master equation that accounts for the effect of binary particle collisions on the suspension motion. In the simplest two-dimensional (2D) version (with no  $y$  direction), the master equation reads

$$\frac{\partial n(z, t)}{\partial t} = \dot{\gamma} \int_{-\infty}^{\infty} [n(z + \frac{1}{2}\Delta - \frac{1}{2}\Delta')n(z - \frac{1}{2}\Delta - \frac{1}{2}\Delta') - n(z)n(z - \Delta)] \Delta d\Delta, \quad (1)$$

where  $\Delta$  and  $\Delta'$  are the pre-collision and post-collision particle offsets. For simplicity, we assume that the interacting particles undergo symmetric transverse displacements. The first term of the integrand on the right-hand side of Eq. (1) corresponds to collisions pushing a particle into the position  $z$  (moving it from  $z + \frac{1}{2}\Delta - \frac{1}{2}\Delta'$ ), and the second term to collisions displacing a particle from the position  $z$ . If the initial and final offsets are the same,  $\Delta = \Delta'$ , the first and second terms of the integrand cancel. In the full three-dimensional (3D) version, an additional integration with respect to the lateral offset  $\Delta y$  would be present [14].

*Collision models M2 and M3* – Based on geometry of binary collisions we introduce a 2D collision model M2,

$$\Delta' = \begin{cases} -\Delta, & 0 < |\Delta| < \kappa_s, \\ \text{sign}(\Delta)\kappa_c, & \kappa_s < |\Delta| < \kappa_c, \\ \Delta, & \kappa_c < |\Delta| < \infty, \end{cases} \quad (2)$$

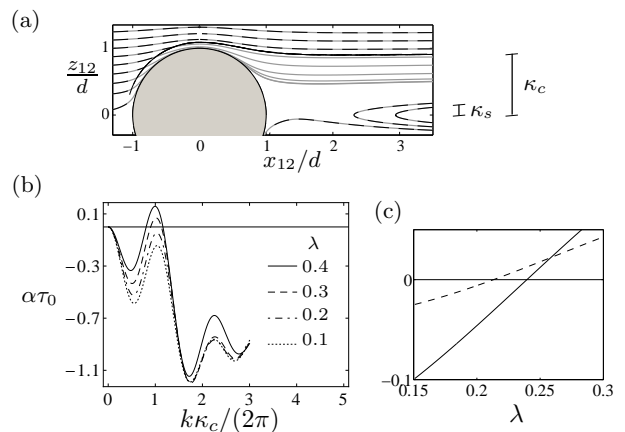


FIG. 3. (a) Pair collisions: relative trajectories for roughness range  $\epsilon/d = 9 \cdot 10^{-2}$  (dashed lines) and  $\epsilon/d = 10^{-3}$  (gray solid). (b) Growth rate  $\alpha$  of small harmonic perturbations vs the wavevector  $k$  for several values of the swapping ratio  $\lambda$  (as labeled) in model M2. (c) Peak value of  $\alpha$  vs swapping ratio  $\lambda$  for model M2 (solid) and M3 (dashed). The growth-rate ratio  $\alpha$  is normalized by the characteristic time  $\tau_0^{-1} = \dot{\gamma} n_0 \kappa_c^D$ , where  $D$  is the dimensionality of the model.

where  $\kappa_s$  is the swapping range and  $\kappa_c$  collision range. For a collision parameter  $\Delta$  smaller than the swapping range  $\kappa_s$ , particle swapping leads to the exchange of transverse particle positions, consistent with the results of our hydrodynamic calculations illustrated in Figs. 1(c) and 3(a). Hence, the two terms of the integrand in Eq. (1) cancel each other. For the collision parameter in the range  $\kappa_s < |\Delta| < \kappa_c$ , particle interaction results in finite particle displacements.

In M3, our 3D model [14], particles on collisional trajectories behave as hard spheres without HI. In the swapping trajectory region  $|\Delta| < \kappa_s$  the particles exchange their transverse positions  $z$  (as in model M2).

*Small perturbation analysis* – We show that the existence of the swapping region  $|\Delta| < \kappa_s$  results in a layering instability, provided that the swapping ratio

$$\lambda = \kappa_s / \kappa_c \quad (3)$$

is sufficiently large. The conditions for a uniform particle distribution  $n_0$  to become unstable can be derived by analyzing small harmonic perturbations  $n(z; t) = n_0 + n_1(t)e^{ikz}$ . For the translationally invariant population-balance models M2 and M3, such Fourier modes evolve exponentially,  $n_1(t) = n_1(0)e^{\alpha t}$ .

Figure 3(b) shows that the growth rate  $\alpha(k)$  has a peak around  $k \approx 2\pi/\kappa_c$ . Since the peak value becomes positive at a critical swapping ratio  $\lambda = \lambda_c$ , the uniform particle distribution is unstable to small perturbations for  $\lambda > \lambda_c$ , leading to formation of particle layers. Fig. 3(b) depicts model M2, but we find that M3 yields a similar behavior.

Figure 3(c) shows the peak values of  $\alpha$  plotted vs. the swapping ratio  $\lambda$  (both for M2 and M3). For M2 the critical swapping ratio is  $\lambda_c = 0.24$ , and for M3 we obtain  $\lambda_c = 0.213$ . Our BMC-HI simulations yield the instability in a similar parameter range.

Based on the dynamics of pair collisions (with HI), the swapping ratio (3) can be controlled in two ways. First, the swapping range  $\kappa_s$  can be changed by varying the wall separation  $H$ . For example, for a particle pair in the middle of the channel, the dimensionless range  $\kappa_s/d$  varies between 0.27 for  $H/d = 5$  and 0.12 for  $H/d = 40$  [11]. Second, the swapping ratio can also be controlled by changing particle roughness, because collision range  $\kappa_c$  diminishes with the decreasing roughness amplitude [15], as shown in Fig. 3(a). We thus predict that by decreasing the magnitude of the particle roughness, we can induce formation of a long-range order in a confined suspension under shear. This prediction is confirmed by our BMC-HI simulations (cf., Fig. 2, where  $\lambda = 0.163$  for  $\epsilon/d = 0.25$  and  $\lambda = 0.23$  for  $\epsilon/d = 0.064$ , based on the mid-channel swapping range  $\kappa_s/d = 0.189$ ).

*Near-wall microstructure* – Further predictions regarding the wall-induced suspension ordering can be obtained when geometrical constraints that disallow particle-wall overlaps are introduced into the population-balance model (1). Figures 4 and 5 show our results for

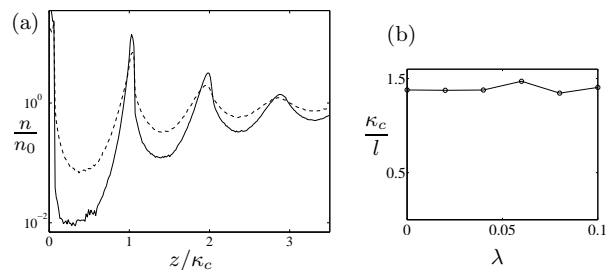


FIG. 4. Long-time near-wall suspension microstructure for subcritical values of swapping ratio  $\lambda$  (model M3) (a) Density profile  $n/n_0$  for  $\lambda = 0$  (dashed line) and  $\lambda = 0.1$  (solid). (b) inverse correlation length  $l^{-1}$  vs  $\lambda$ .

model M3 with such constraints. We consider a system with a large wall separation  $H/\kappa_c = 60$  to emphasize two important regimes of suspension behavior: subcritical (Fig. 4) and supercritical (Fig. 5).

In both regimes we observe formation of a wall-induced layered order, but the evolution and extent of the layered microstructure is regime-specific. For subcritical values of the swapping ratio (3), the microstructure appears only in the near-wall domain, whereas for supercritical values the layered structure propagates from the wall into the bulk of the suspension.

*Subcritical regime* – Figure 4(a) shows the subcritical microstructure for  $\lambda = 0$  (no swapping) and  $\lambda = 0.1$  (significant swapping). In both cases several particle layers form near the wall due to the excluded-volume effect.

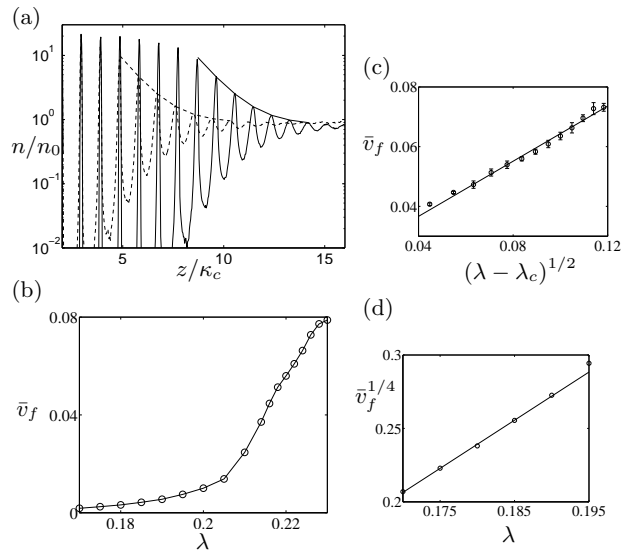


FIG. 5. Near-wall suspension microstructure for supercritical values of swapping ratio  $\lambda$  (model M3). (a) Density profile at times  $t_1/\tau_0 = 1250$  (dashed line) and  $t_2/\tau_0 = 2500$  (solid line) for swapping ratio  $\lambda = 0.18$  and channel width  $H/d = 60$ . Characteristic time  $\tau_0 = 1/(n_0\gamma\kappa_c^3)$ . (b) Normalized propagation velocity  $\bar{v}_f = v_f\tau_0/\kappa_c$ . Near critical scaling behavior of  $\bar{v}_f$  for two cases: (c)  $\lambda \gtrsim \lambda_c$ , and (d)  $\lambda \gtrsim \lambda_w$ .

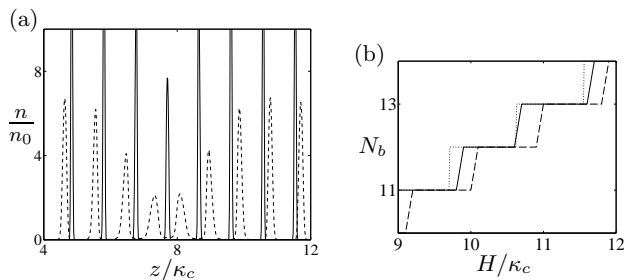


FIG. 6. Layer restructuring for supercritical swapping ratio  $\lambda = 0.24$  (model M3). (a) Merging of two central layers when the width is incommensurate  $H/\kappa_c = 15.4$ ; intermediate time (dashed line), long time (solid). (b) Number of layers vs normalized channel width: maximal number during evolution (solid); steady state (dashed); estimate based on the wavelength of the most unstable Fourier mode (dotted).

The correlation length  $l$  of this local layered structure is insensitive to the value of  $\lambda$  in the whole subcritical regime [cf., Fig. 4(b)]. However, for  $\lambda = 0$  the layers are not sharply defined, with many particles in the valleys between the density peaks. For  $\lambda = 0.1$  the layers are much sharper. Thus the ST mechanism influences the form but not the extent of the subcritical microstructure.

*Supercritical regime* – In the supercritical regime (cf. Fig. 5) the wall-induced microstructure propagates from the wall with velocity  $v_f$ , forming a growing number of particle layers, as shown in Fig. 5(a). In a fully developed microstructure the layers are well separated, and particle jumps between layers are rare [cf., Fig. 1(d)].

The propagation velocity  $v_f$  of the layered structure in this regime [cf. Fig. 5(b)] is an increasing function of  $\lambda$ , with two distinct dynamical domains. For  $\lambda > \lambda_c$  (suspension unstable to small perturbations),  $v_f$  rapidly increases with the swapping ratio, showing a power law critical behavior  $v_f \sim (\lambda - \lambda_c)^{1/2}$  [cf. Fig. 5(c)]. In the domain  $\lambda_w < \lambda < \lambda_c$  the suspension is stable to small perturbations, but unstable to the *large perturbation* caused by the wall. In this regime, the data can be well fitted to the power law  $v_f \sim (\lambda - \lambda_w)^\beta$  with  $\lambda_w \approx 0.11$  and  $\beta \approx 4$  [cf. Fig. 5(d)]. Due to the large value of the exponent  $\beta$ , the propagation velocity  $v_f$  is practically zero for  $\lambda \lesssim 0.16$ .

The layer separation in the propagating microstructural fronts may be incommensurate with the wall separation. In such cases the two mid-channel layers merge, as depicted in Fig. 6(a). After such suspension restructuring, the width of the density peaks significantly decreases. Note that the initial number of layers agrees fairly well with our prediction based on the wavelength of the most unstable Fourier mode [cf. Fig. 6(b)].

*Conclusions* – The ST mechanism significantly alters the suspension microstructure in a confined Couette flow by inducing layering. Previously (solving a long-standing paradox [16]), we have demonstrated that swapping tra-

jectories cause the anomalous enhancement of hydrodynamic diffusion, and that they stabilize particle chains in microfluidic channels [11]. The layering behavior identified and analyzed here adds to the growing evidence that a seemingly subtle ST effect has far-reaching consequences in confined particulate flows.

Our direct numerical simulations indicate that swapping trajectories significantly influence a variety of confined systems, including suspensions at higher concentrations [14] and flow-driven particle monolayers described in [7]. Since such monolayers (in the disordered state) have a similar structure to the layers observed experimentally in [13], we conclude that the ST effect has significant implications for suspension dynamics. In suspensions with nonzero inertial forces [17] and in viscoelastic fluids, swapping (reversing) trajectories occur even without confinement, so the ST mechanism is likely to affect suspension microstructure also in such flows.

Finally, we note that the suspension behavior described in our study significantly differs from the dynamics of a dilute gas. In a gas, binary collisions always produce a homogeneous equilibrium state, according to Boltzmann’s H-theorem. By analogy, it is assumed that binary collisions in suspension flows always lead to a diffusive behavior that results in relaxation of density fluctuations. Here we report that *uncorrelated binary collisions* produce inhomogeneous layered microstructure.

We acknowledge financial support by NSF grant CBET 1059745 (JB), Ministerio de Innovación y Ciencia grant RYC-2008-03650 (MZG), and Polish Ministry of Science and Higher Education Grant No. N N501 156538 (EW).

- 
- [1] T. Thorsen, R. W. Roberts, F. H. Arnold, and S. R. Quake, Phys. Rev. Lett. **86**, 4163 (2001).  
I. Cohen, T. G. Mason, and D. A. Weitz, Phys. Rev. Lett. **93**, 046001 (2004).
  - [2] A. Komnik, J. Harting, and H. Herrman, J. Stat. Mech.: Theory Exp. p. P12003 (2004).  
K. Yeo and M. Maxey, Phys. Rev. E **81**, 051502 (2010).  
X. Xu, S. Rice, A. Dinner, X. Cheng, and I. Cohen, in *2011 APS March Meeting, March 21–25, 2011, Dallas, TX* (2011).
  - [3] B. Cui, H. Diamant, B. Lin, and S. A. Rice, Phys. Rev. Lett. **92**, 258301 (2004).
  - [4] T. Beatus, T. Tlusty, and R. Bar-Ziv, Nature Physics **2**, 743 (2006).  
T. Beatus, R. Bar-Ziv, and T. Tlusty, Phys. Rev. Lett. **99**, 124502 (2007).
  - [5] M. Baron, J. Bławdziewicz, and E. Wajnryb, Phys. Rev. Lett. **100**, 174502 (2008).
  - [6] H. Eral, D. van den Ende, F. Mugele, and M. Duits, Phys. Rev. E **80**, 061403 (2009).
  - [7] J. Bławdziewicz, R. H. Goodman, N. Khurana, E. Wajnryb, and Y. N. Young, Physica D **239**, 1214 (2010).
  - [8] B. Cui, H. Diamant, and B. Lin, Phys. Rev. Lett. **89**, 188302 (2002).

- [9] S. Navardi and S. Bhattacharya, *Phys. Fluids* **22**, 103306 (2010).
- [10] S. Bhattacharya, J. Bławdziewicz, and E. Wajnryb, *J. Fluid Mech.* **541**, 263 (2005).
- [11] M. Zurita-Gotor, J. Bławdziewicz, and E. Wajnryb, *J. Fluid Mech.* **592**, 447 (2007).
- [12] G. Bossis, A. Meunier, and J. D. Sherwood, *Phys. Fluids A* **3**, 1853 (1991).
- [13] I. Cohen and X. Cheng, in *2011 APS March Meeting, March 21–25, 2011, Dallas, TX* (2011).
- [14] See Supplemental Material at <http://link.aps.org/> for description of BMC method, definition of collision model M3 and for movies of confined suspension dynamics.
- [15] F. da Cunha and E. Hinch, *J. Fluid Mech.* **309**, 211 (1996).
- [16] I. E. Zarraga and D. T. Leighton, *Phys. Fluids* **14**, 2194 (2002).
- [17] D. R. Mikulencak and J. F. Morris, *J. Fluid Mech.* **520**, 215 (2004).